Westinghouse Non-Proprietary Class 3

WCAP-15617
Revision 0

Integrity Evaluation for Future Operation Virgil C. Summer Nuclear Plant: Reactor Vessel Nozzle to Pipe Weld Regions

Westinghouse Electric Company LLC

WCAP-15617

Integrity Evaluation for Future Operation: Virgil C. Summer Nuclear Plant Reactor Vessel Nozzle to Pipe Weld Regions

Warren H. Bamford
Lee Tunon-Sanjur
Robert Hsu

December 2000

Reviewer: D. Bhowmick
D. C. Bhowmick
Structural Mechanics Technology

Approved: S.A. Swamy
S. A. Swamy, Manager
Structural Mechanics Technology

Westinghouse Electric Company LLC
P.O. Box 355
Pittsburgh, PA 15230-0355

TABLE OF CONTENTS

LIST OF TABLES

LIST OF FIGURES

1 INTRODUCTION

In early October 2000 the V. C. Summer Plant shut down for a normal refueling outage, and began a walkdown to search for boron deposits, as is done to begin each outage. During the walkdown, significant boron deposits were discovered in the vicinity and on the Loop "A" outlet nozzle to pipe weld. Insulation was removed, and leakage monitoring records were searched.

Leakage records showed a nearly constant value of 0.3 GPM unidentified leakage from all sources, well below the plant technical specification limit of 1.0 GPM.

The design geometry of the nozzle to pipe weld is shown in Figure 1-1.

Ultrasonic tests performed on the pipe from the inside surface revealed a single axial flaw near the top of the pipe. The flawed region has been removed, and a new spool piece is to be welded in place, returning this region to its original condition, with a weld material much more resistant to cracking, Alloy 52.

The purpose of this report is to support the return to service of the V. C. Summer plant. Due to the potential cracking susceptibility of the nozzle to pipe welds which were not replaced, a flaw evaluation has been carried out using the rules of ASME Section XI, paragraph IWB 3640.

In addition, an assessment was made of the requirements for demonstration of leak before break will be provided, along with a justification for continued applicability of that concept.

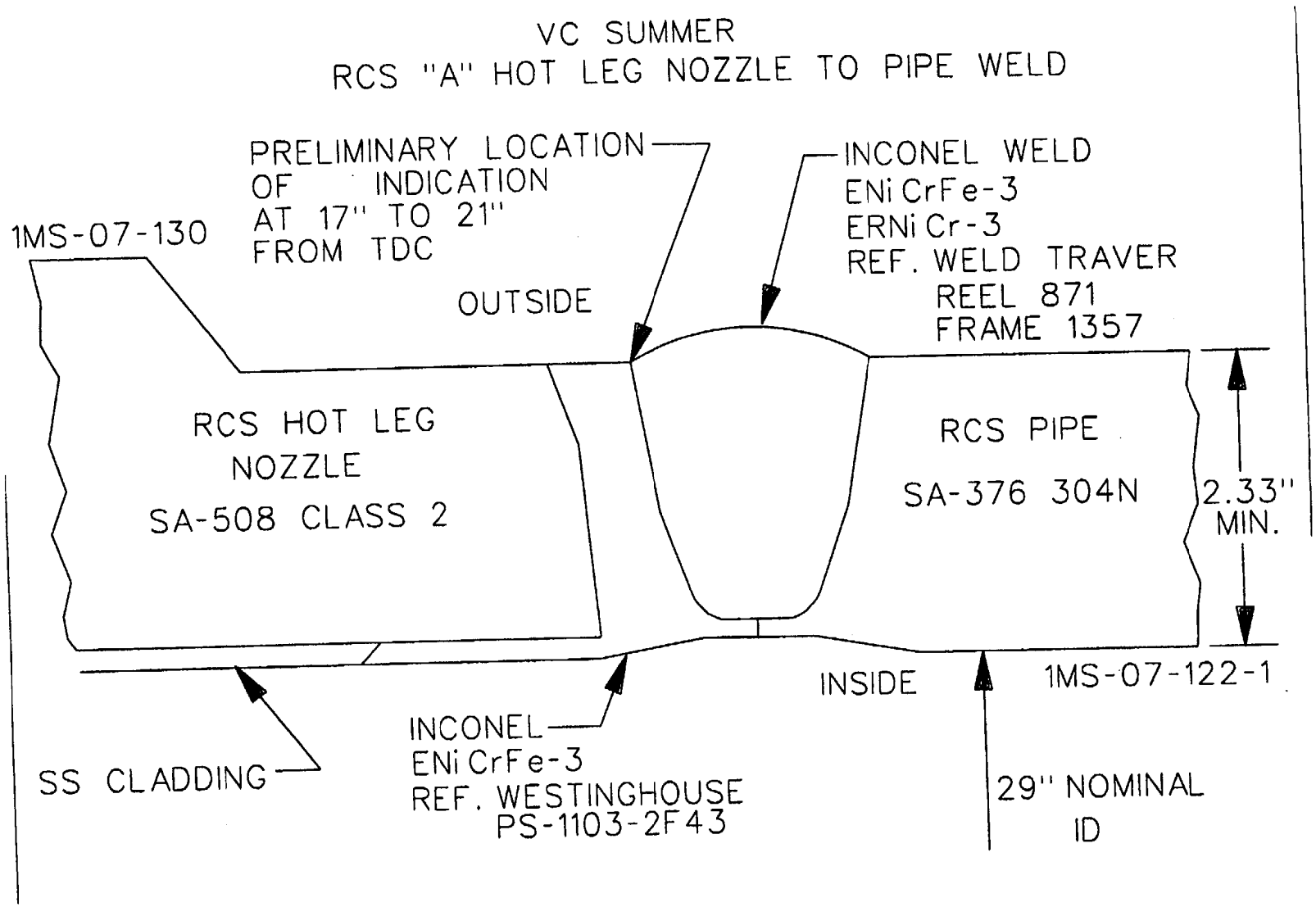

Figure 1-1 Geometry of Nozzle to Pipe Weld Region – V. C. Summer

2 GEOMETRY, MATERIALS AND LOADINGS

The V. C. Summer reactor vessel was fabricated by Chicago Bridge and Iron Company, and began service in 1983. The reactor vessel nozzle, which is a ferritic forging, SA508 Class 2, nozzle was buttered with Alloy 182 weld metal before heat treatment. It was then welded to the main loop piping in the field with Alloy 82 weld metal. The mechanical properties of 82 and 182 are essentially the same. The main loop piping is forged SA 376 Type 304N stainless steel, and the nozzle to pipe weld configuration and materials are shown in Figure 1-1.

The material properties of the nozzle to pipe weld materials are provided in Table 2-2. Properties were determined at both room temperature and normal operating temperature of 619°F. The minimum values were used for the flaw stability calculations, and the average values were used for the leak rate calculations for the stainless steel. For Alloy 182, only average values were available, so they were used for both calculations.

The calculations to be discussed here considered all the appropriate loadings, including dead weight, thermal expansion and pressure. For critical flaw size calculations, the seismic loads were also included. For the leak rate calculations, the normal loads from reference 1 were used.

The loadings for both the governing normal/upset condition and the governing emergency/faulted condition were updated to include all design changes to the system. Such changes include the following:

- Steam generator replacement and uprating
- Steam generator snubber elimination
- Steam generator center of gravity and weight revisions

The loadings in the reactor vessel to pipe weld region of loop A are provided in Table 2-1.

The forces and moments for each condition were obtained from calculations previously performed by Westinghouse. The stress intensity values were calculated using the following equations:

$$SI = P_m + P_b$$

$$SI = \frac{F_x}{A} + \frac{1}{Z}[M_y^2 + M_z^2]^{0.5}$$

where

F_x	=	axial force component (membrane)
M_y, M_z	=	moment components (bending)
A	=	cross-section area
Z	=	section modulus

The section properties A and Z at the weld location were determined based on the following pipe dimensions: outside diameter of 33.90 inches, wall thickness of 2.345 inches. The following load combinations were used.

A. Normal/Upset - Primary Stress

Pressure + Deadweight $\pm$ OBE

B. Emergency/Faulted - Primary Stress

Pressure + Deadweight $\pm$ SSE

C. Expansion Stress - Secondary Stress

i) Normal Thermal

ii) Upset Thermal

D. Normal/Upset - Total Stress

i) Pressure + Deadweight + OBE + Normal Thermal

ii) Pressure + Deadweight + Upset Thermal

E. Emergency/Faulted - Total Stress

i) Pressure + Deadweight + SSE + Normal Thermal

ii) Pressure + Deadweight + Faulted Thermal + Break Loads

Table 2-1 Loads for Virgil Summer		
Condition	**Axial Load (kips)**	**Bending Moment (in-kips)**
Dead weight	.24	1007.8
Thermal	-117.9	12538.4
OBE	301.1	6621.7
SSE	451.7	9932.5

Pressure = 2250 psi

Table 2-2 Material Properties						
		Yield Strength (ksi)		**UTS (ksi)**		**Youngs Mod. ($x10^6$ psi)**
	Material	**RT**	**619F**	**RT**	**619F**	
Hot Leg Piping	304 Forging [1]	[				
RV Nozzle	508 Class 2 [12] Forging					
Weld	Alloy 182 [13]					]^{a,c,e}

RT = room temperature
UTS = ultimate tensile strength
*** minimum values**

3 INSPECTION FINDINGS AND ROOT CAUSE DETERMINATION

Automated nondestructive examinations were performed on all six V. C. Summer reactor vessel hot leg and cold leg nozzle to pipe weld inside surfaces from November 4 through November 7, 2000. Scanning was performed with a single WesDyne SUPREEM robot, upper platform configuration, seated on the ledge of the reactor vessel flange.

Examinations included automated Ultrasonic Testing with data acquired and analyzed on the WesDyne Paragon system. Automated Eddy Current Testing was employed as a complimentary NDE technique with data acquired and analyzed on the Intraspect system. A high-resolution camera system was also attached to the nozzle end-effector for evaluation of the pipe weld inside surface. Examinations and qualification activities were performed by WesDyne and witnessed by V. C. Summer technical representatives and consulting utility NDE specialists, EPRI NDE specialists, USNRC resident, regional and consulting NDE specialists and the V. C. Summer plant ANII.

Technique qualification was performed at the site on an EPRI-supplied Safe-End Test Block (Specimen 19-36-2.5-PWR-316-BN). Two flaws with the shallowest depth were selected for eddy current technique qualification (the flaw "F" circumferentially oriented, and the flaw "K" axially oriented). The eddy current technique was able to detect and accurately map the surface contour (length) for both flaws.

The results of both the eddy current and UT examinations are documented in Reference [4].

The results of the UT inspections showed only one flaw, and that was located in Loop A, and had penetrated the wall. No other indications were identified by UT in any of the nozzle to pipe welds in any of the loops.

Some eddy current indications were identified, and a summary of these results is provided in Table 3-1. Only eddy current indications with length over 0.25 inches have been included here. Several of the eddy current indications found in the Loop A weld have been verified by actual measurement, and these are marked with an asterisk in the table. The largest indication that was verified to be a crack was located at 250 degrees, and had a length of 0.75 inch and depth of 0.615 inch.

The eddy current indications in Table 3-1 represent groups of responses, rather than single eddy current hits. These indications were selected from the larger group of results presented in reference [4], on the basis of the indicated length exceeding 0.25 inches. Experience indicates that the shorter indications are typically scratches, surface anomalies, or very short and shallow cracks. Several indications were also ignored as uncharacteristic responses because no orientation could be determined.

A metallurgical investigation [5] was conducted on the ring segment removed from the hot leg A nozzle to pipe weld, and led to a number of key conclusions. The cracking origin on the inside surface was not identified, but the mechanism was identified as interdendritic stress corrosion cracking.

Destructive examination of the ring segment in the regions of the eddy current indications has been carried out [5]. The largest of the eddy current indications (other than the through-wall flaw) has been confirmed to be an axial crack with a length of 0.75" and depth = 0.615". A second indication is a circumferential crack, with length of 1.6" and depth = 0.2", confined entirely to the Alloy 182 cladding. A number of smaller indications were also characterized, as shown in Table 3-1.

An important consideration in the case of stress corrosion cracking is the temperature, as both crack initiation resistance and crack growth resistance increase significantly with lower temperatures. This means that the hot legs will be significantly more likely have cracks than the cold legs. The "A" hot leg weld has been replaced, so the other two hot legs merit attention. The UT examinations showed no indications in these other hot legs, but there is one eddy current indication of note in loop "C", and there are three in loop "B". It is clear from Table 3-1 that there are few if any indications of concern in these other loops, but nonetheless, postulated flaws will be evaluated to determine the flaw tolerance of these regions.

Table 3-1 Indications in V. C. Summer RV Nozzle to Pipe Weld Regions					
Loop	**Leg**	**Circ. Location/ Orientation**	**Length (Eddy Current)**	**Length/Depth* (as measured)**	**Aspect Ratio**
[					
					]^{a,c,e}

*Verified by destructive examination.

4 SUBCRITICAL CRACK GROWTH

In applying the ASME Code Section XI [2] acceptance criteria, the final flaw size (a_f) used is defined as the flaw size to which the detected flaw is calculated to grow until the next inspection period. Both fatigue and stress corrosion crack growth will be considered.

4.1 FATIGUE CRACK GROWTH

To determine the fatigue crack growth in each piping weld region, an analysis was performed for the actual location of interest. The loadings used were thermal and deadweight piping loads, pressure, thermal transient loads, and residual stresses.

The analysis procedure involves postulating an initial flaw at each specific region at start of life and predicting the flaw growth due to an imposed series of loading transients. The input required for a fatigue crack growth analysis is basically the information necessary to calculate the parameter ΔK_I (range of stress intensity factor), which depends on the geometry of the crack, its surrounding structure and the range of applied stresses in the crack area. Once ΔK_I is calculated, the growth due to a particular stress cycle can be calculated by an equation developed from references 15 and 16. This incremental growth is then added to the original crack size, and the analysis proceeds to the next cycle or transient. The procedure is continued in this manner until all of the analytical transients known to occur in the 10, 20 or 30 years of operation have been analyzed.

The transients considered in the analysis are the design transients contained in the equipment specification, as shown in Table 4-1. The transient occurrences are conservative relative to those recorded by the transient monitoring system WESTEMS [14]. These transients were distributed equally over the plant design life, with the exception that the preoperational tests are considered first.

The fatigue crack growth results for postulated axial and circumferential flaws are shown in Table 4-2, for range of flaw sizes. As seen in the table, the crack growth is very small, even for 40 years service. As will be seen below, crack growth due to stress corrosion cracking is the limiting mechanism of subcritical growth.

4.2 STRESS CORROSION CRACK GROWTH

The most important mode of subcritical crack growth is PWSCC, which was the reported mechanism from the root cause analysis of the crack in the loop A hot leg. Recently an experimental program was carried out to measure crack growth rates in Alloy 182, and the results were reported in Reference 6. Although crack growth rate tests were not conducted on Alloy 82, the behavior is expected to be similar. Seventeen specimens from three different welds were tested, and the results showed reasonably consistent growth rates between the three welds.

[

]a,c,e

Crack growth due to the PWSCC was calculated for both axial and circumferential flaws, using the steady-state stresses discussed in Section 2. For axial flaws, this includes pressure and residual stresses, while for circumferential flaws the appropriate stresses are pressure, thermal, deadweight, and residual stresses. The residual stresses were estimated using Reference 3, which is the technical basis of the flaw evaluation process for piping in Section XI. The recommended values for residual stress are presented in Figure 4-3.

4.2.1 Axial Flaws

[

]a,c,e There are four axial flaws which were destructively examined from loop A, and the length is naturally limited by the width of the weld, which is about 2.5 inches. The crack growth results from postulated axial flaws are presented in Figure 4-4.

4.2.2 Circumferential Flaws

[

]^{a,c,e}

In estimating the flaw shape for the circumferential flaws, several considerations are necessary. The measured shapes of known flaws would be most reliable, but there are no natural circumferential flaws measured. Therefore, several flaw shapes were evaluated.

[

]^{a,c,e}

The crack growth results for postulated circumferential flaws are shown in Figures 4-5 through 4-7.

Table 4-1 Summary of Primary System Transients – Reactor Coolant System (RCS)		
Transient Number	**Transient Identification**	**Cycles**
1	Partial loss of flow	80
2	Inadvertent S.I.* Actuation	60
3	Heatup	200
4	Cooldown	200
5	Unit loading at 5% per minute	18300
6	Unit unloading at 5% per minute	18300
7	10% step load increase	2000
8	10% step load decrease	2000
9	Large step load decrease with steam dump	200
10	Feedwater cycling at hot shutdown	2000
11	Loop out-of-service, normal loop startup	70
12	Loop out-of-service, normal loop shutdown	80
13	Reactor trip from full power – no cooldown	230
14	Reactor trip from full power – cooldown, no S.I.*	160
15	Reactor trip from full power – cooldown and S.I.*	10
16	Inadvertent startup of an inactive loop – inactive loop	10
17	Inadvertent startup of an inactive loop – active loop	10
18	Small LOCA (E/F)*	5
19	Small steam line break (E/F)*	5
20	Complete loss of flow (E/F)*	5
21	Turbine roll test – heat up	10
22	Turbine roll test – cooldown	10
23	Loss of load	80
24	Control rod drop	80
25	Loss of power	40
26	Inadvertent RCS depressurization	20
27	Unit loading – 15%	500
28	Unit unloading – 15%	500
29	Steady state fluctuation	150000
30	Feedwater Heaters Out of Service	80
31	OBE	400

*NOTE: S.I. = Safety Injection
E/F = Emergency/Faulted Condition

Table 4-2 Results of Fatigue Crack Growth: Outlet Nozzle to Pipe Weld				
Circumferential Flaw (Flaw length 6 times depth)				
Initial Flaw Depth (in)	Flaw Depth (in.) After			
	10 years	20 years	30 years	40 years
0.200	0.2053	0.2110	0.2169	0.2233
0.400	0.4197	0.4409	0.4632	0.4875
0.600	0.6379	0.6796	0.7244	0.7730
0.800	0.8528	0.9077	0.9633	1.0195
	Axial Flaw (Flaw length 2 times depth)			
0.200	0.2000	0.2000	0.2000	0.2000
0.400	0.4000	0.4000	0.4001	0.4001
0.600	0.6000	0.6000	0.6001	0.6001
0.800	0.8001	0.8001	0.8001	0.8001

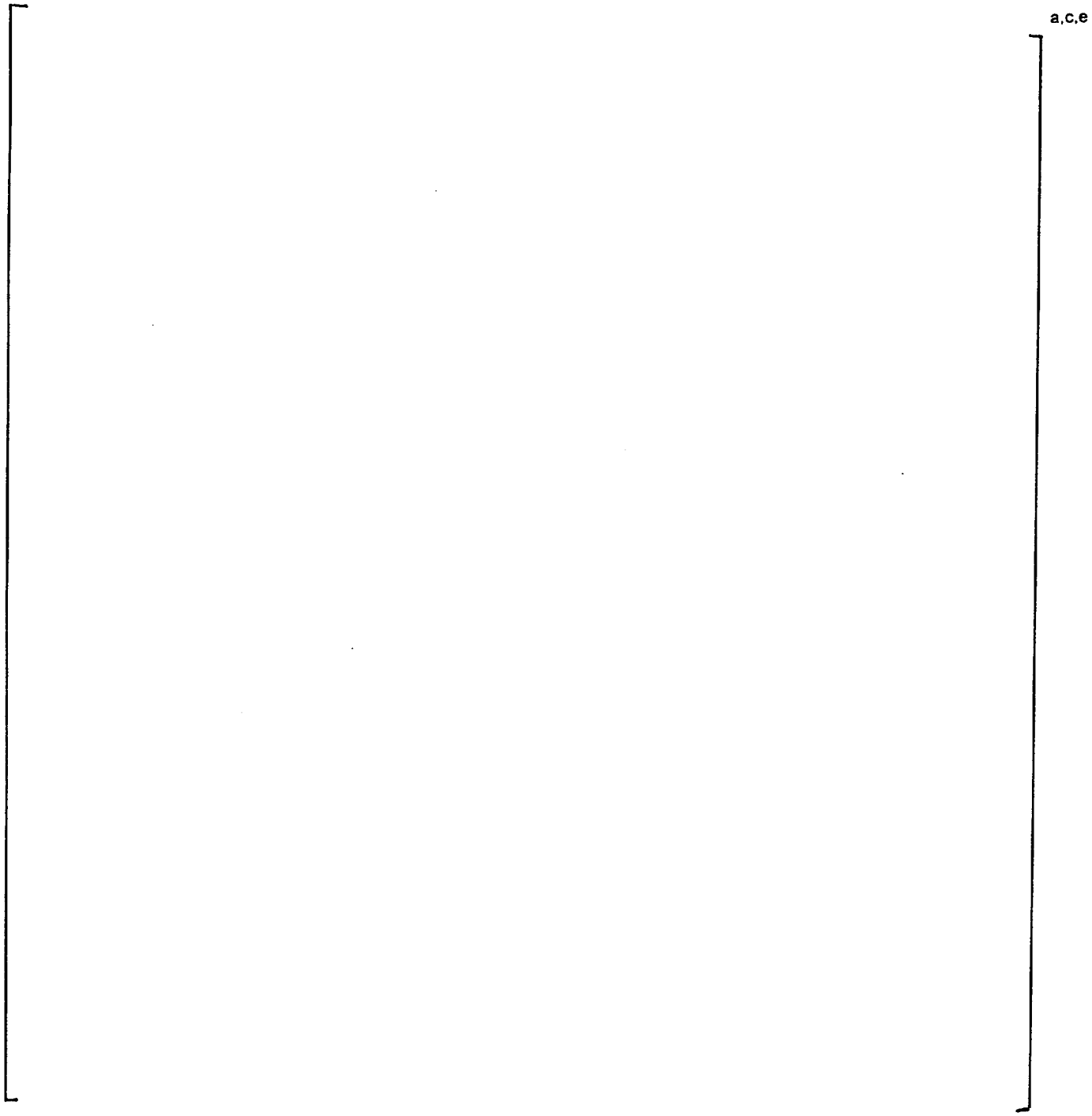

Figure 4-1 Effects of Temperature on Growth Rates of Alloy 182 (K = 22 – 26 Mpa $\sqrt{m}$) [6]

a,c,e

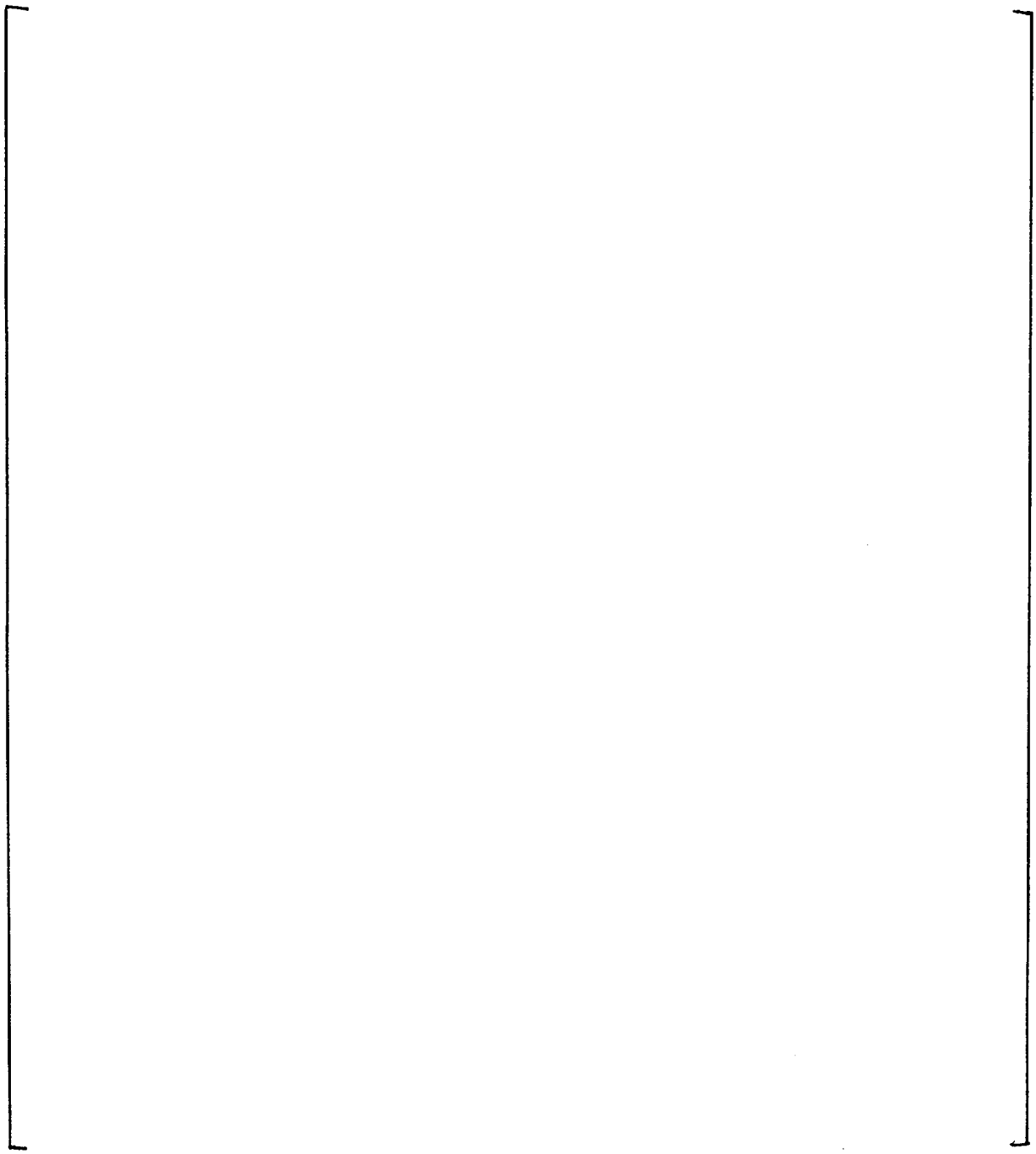

Figure 4-2 Crack Growth Model for Alloy 182 in PWR Environment with Available Data [6] Note that the majority of the results are for cracks oriented along the dendrites

Wall Thickness	Through-Wall Residual Stress[1]	
	Axial	Circumferential[2]
< 1 inch	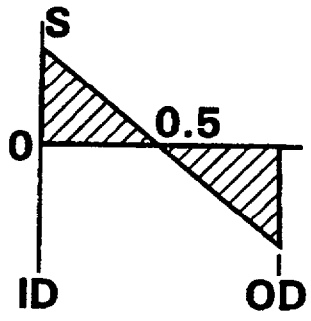	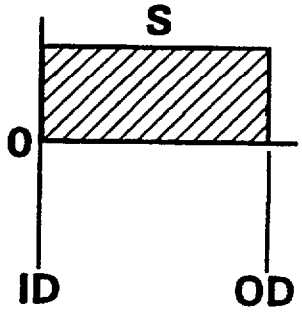
≥ 1 inch	See Note 3	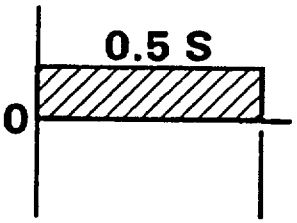

[1] S = 30 ksi

[2] Considerable variation with weld heat input.

[3] $\sigma = \sigma_i [1.0\text{-}6.91(a/t) + 8.69(a/t)^2\text{-}0.48(a/t)^3\text{-}2.03(a/t)^4]$

σ_i = stress at inner surface (a = 0)

Figure 4-3 Recommend Axial and Circumferential Residual Stress Distributions for Austenitic Stainless Steel Pipe Welds [3]

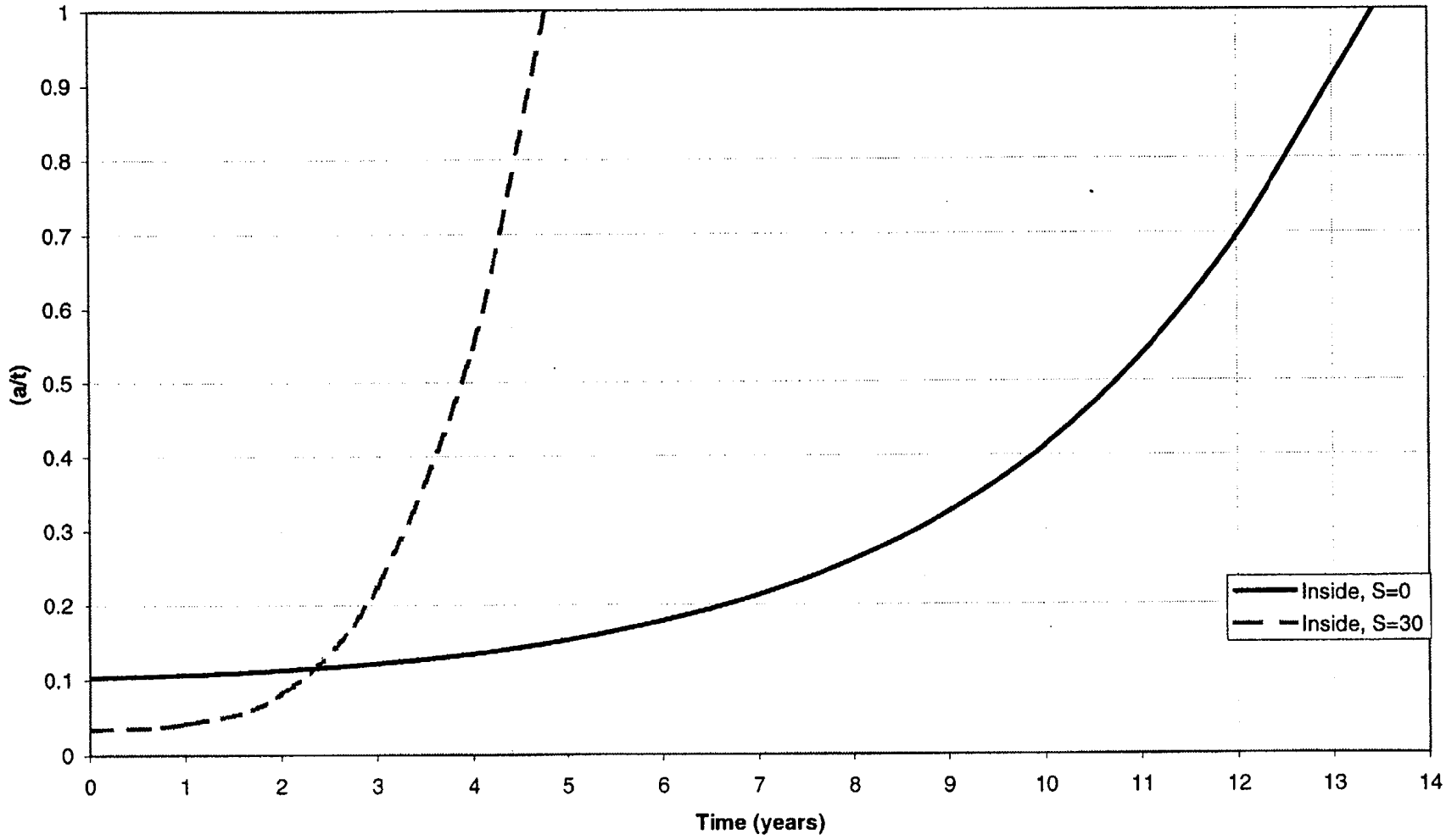

Figure 4-4 Crack Growth Predictions vs. Time for Postulated Axial Flaws, Aspect Ratio 2:1

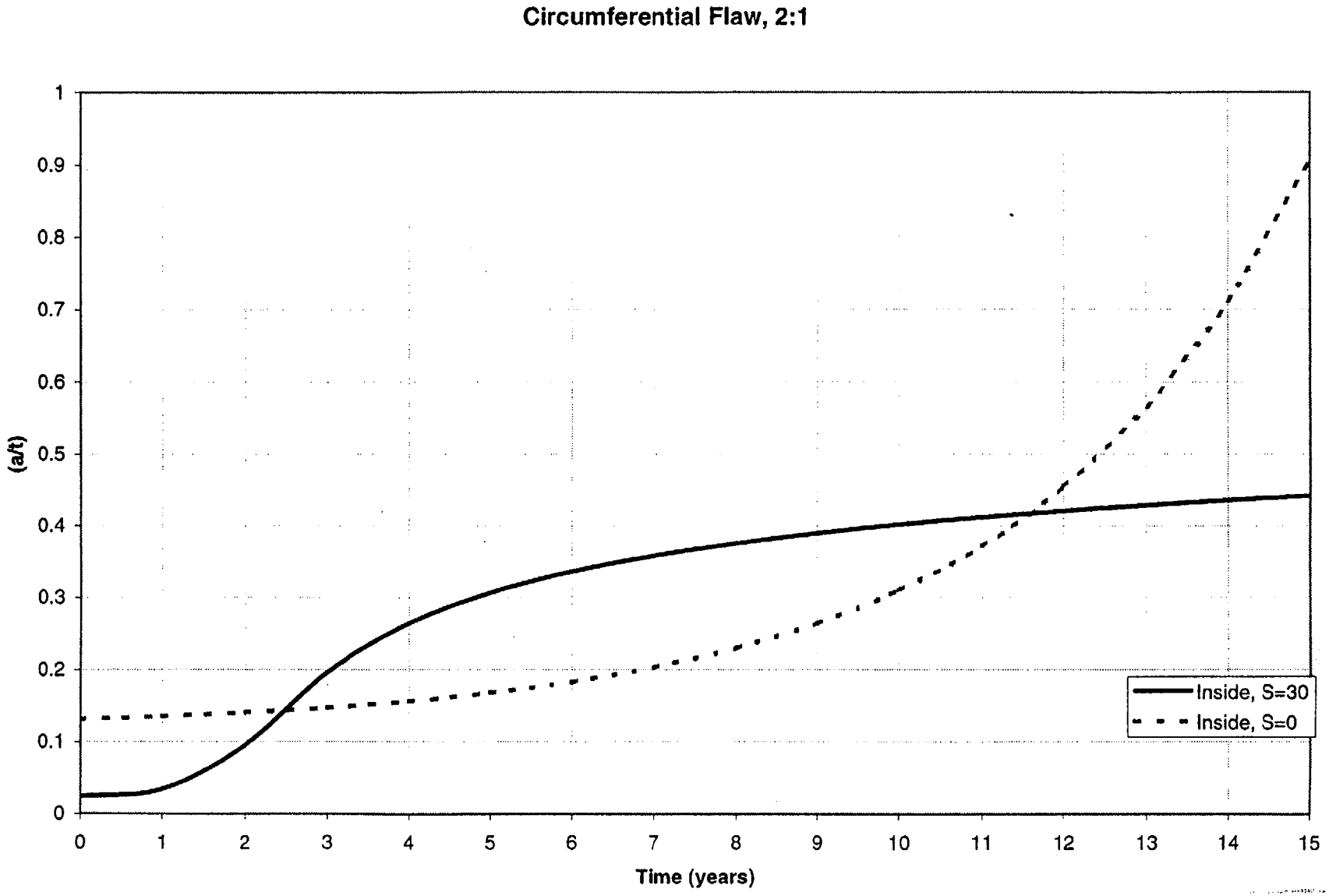

Figure 4-5 Crack Growth Predictions vs. Time for Postulated Circumferential Flaws, Aspect Ratio 2:1

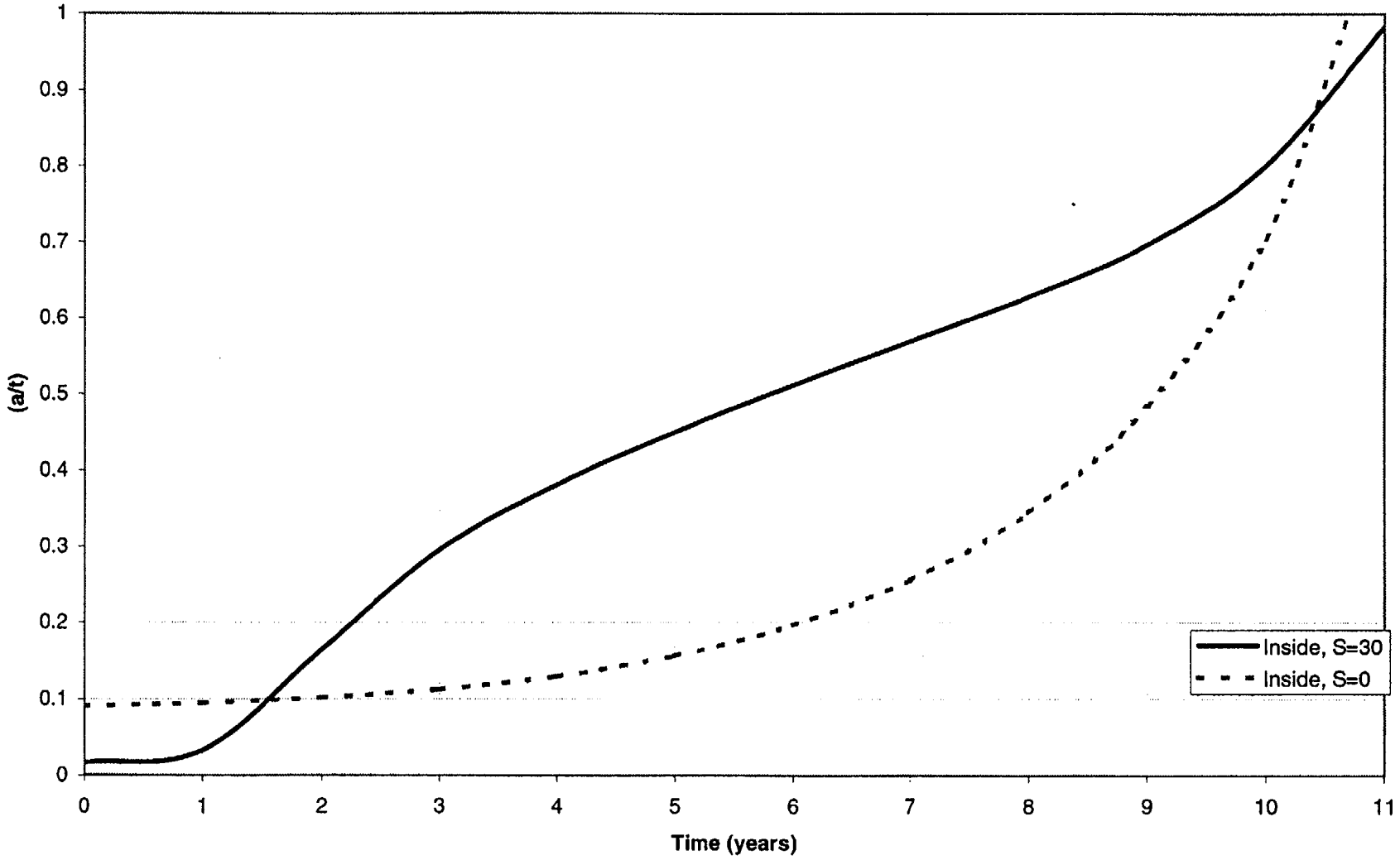

Figure 4-6 Crack Growth Predictions vs. Time for Postulated Circumferential Flaws, Aspect Ratio 3:1

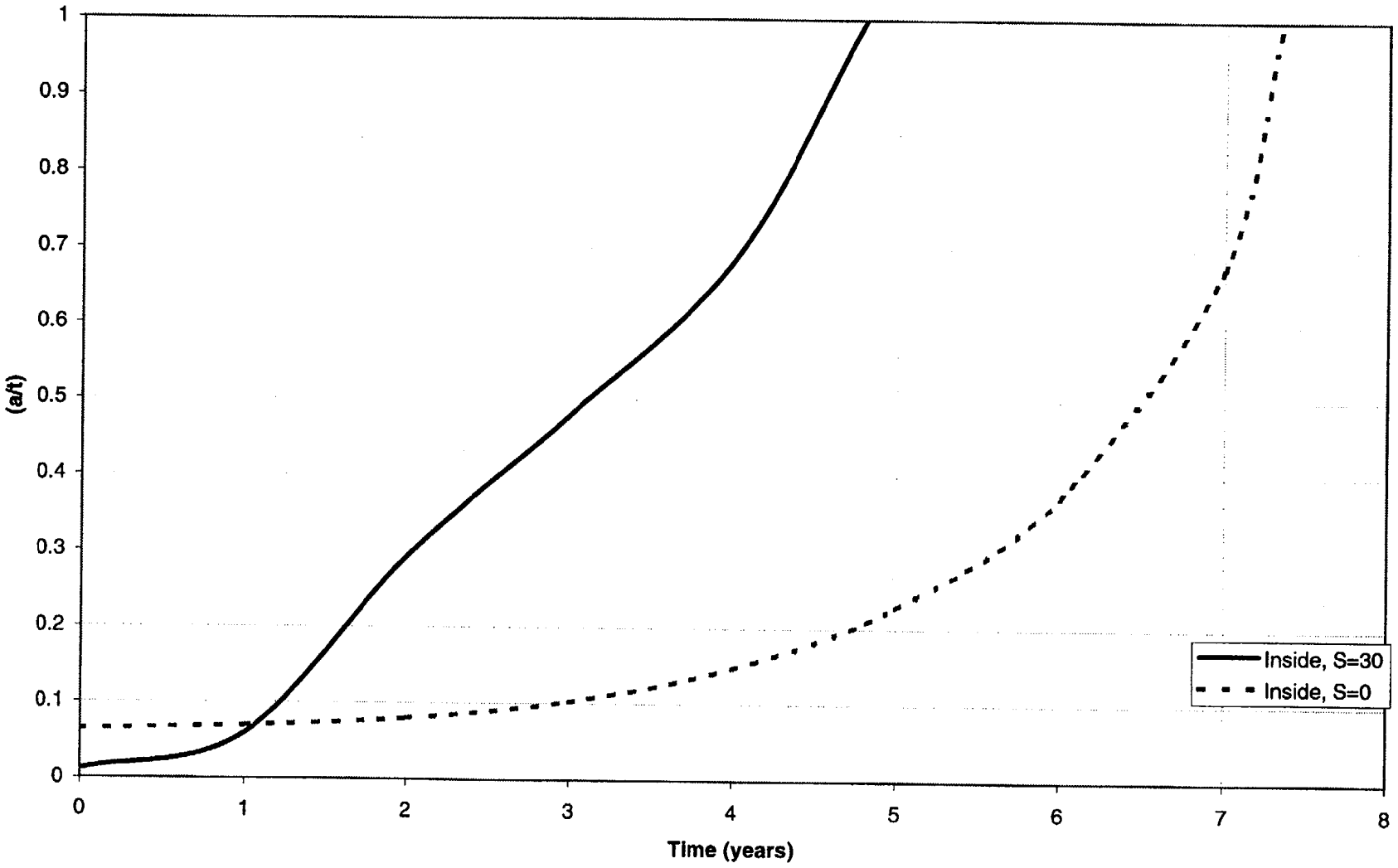

Figure 4-7 Crack Growth Predictions vs. Time for Postulated Circumferential Flaws, Aspect Ratio 6:1

5 ASME CODE ALLOWABLE FLAW SIZE FOR FUTURE OPERATION

The evaluation procedures and acceptance criteria for indications in austenitic stainless piping are contained in paragraph IWB 3640 of ASME Section XI [2]. The evaluation procedure is applicable to all the materials within $\sqrt{rt}$ from the weld centerline (where r = the pipe nominal outside radius, and t is the wall thickness).

The evaluation process begins with a flaw growth analysis, including the requirements for fatigue and stress corrosion cracking. The methodology for the fatigue crack growth analysis is described in detail in Section 4, along with that for stress corrosion cracking.

Next, the calculated maximum flaw dimensions for the specified interval are compared with the maximum allowable flaw dimensions for both normal operating conditions and emergency and faulted conditions, to determine acceptability for continued service. Both circumferentially and axially oriented flaws are considered.

In paragraph IWB 3640 of the Code [2], the allowable flaw sizes are defined in the tables based on failure load safety margins. These margins are 2.77 for normal and upset conditions and 1.39 for emergency and faulted conditions.

Axial Flaws

Using the requirements of IWB 3640 of Section XI, and the stresses discussed in Section 2, an allowable flaw depth was calculated for an axial flaw, length to depth ratio 2:1. This flaw shape conservatively bounds the average flaw shapes determined destructively in the loop "A" weld region, as discussed earlier in Section 4.2. The allowable depth was found to be 75 percent of the wall thickness.

Using Figure 4-4, the allowable time to reach this depth can be easily determined once the initial depth is known. [

]^{a,c,e}

Referring to Figure 4-4, the time predicted to elapse until the allowable depth of 75 percent of the wall is reached would be 3.2 years. Crack growth in the cold leg nozzles would be predicted to be an order of magnitude slower, but there are no axial indications in any of the cold legs.

Circumferential Flaws

The allowable depth for a circumferential flaw was determined in a similar manner to that used for an axial flaw, using IWB 3640 of Section XI. Three different flaw shapes were postulated here, and the allowable depth for each was found to be 75 percent of the wall thickness. [

]^{a,c,e} The postulated depth will depend on the flaw shape assumed, so each evaluation will be described separately.

[

]^{a,c,e}

Conservatisms

This evaluation has considered the possibility of additional flaws in the primary loops of the V.C. Summer plant, even though no such flaws have been identified by UT. The calculated crack growth due to PWSCC has used a conservatively constructed crack growth law, along with bounding residual stress values. The assumed flaw shapes bound those actually characterized by destructive examination of the eddy current indications found in loop "A". The eddy current indication lengths were used in evaluating postulated flaws in the other legs. Table 3-1 shows that for short flaws (0.5 inches or less) the eddy current results tend to overpredict the flaw length.

Summary

Stress corrosion crack growth calculations have been carried out for a series of postulated flaws in the main loop of the V.C. Summer Nuclear Plant. Results show that the predicted flaw sizes will remain in compliance with the requirements of Section XI for a period of at least three years.

6 ASSESSMENT OF COMPLIANCE WITH THE REQUIREMENTS OF LEAK BEFORE BREAK

Westinghouse performed analysis for the Leak-Before-Break (LBB) of Virgil C. Summer primary loop piping in 1992. The results of the analysis was documented in WCAP-13206 [9] and approved by the NRC in a letter dated January 11, 1993 [10]. Westinghouse also performed an evaluation of LBB of Virgil C. Summer primary loop piping in 1993 to account the effects of Steam Generator Replacement/Uprating program and the results were documented in WCAP-13605 [11].

Westinghouse performed a LBB evaluation of the primary loop piping of Virgil C. Summer primary loop piping in 1997 due to the Steam Generator (SG) snubber elimination program. Recently an evaluation was performed to account the combined effects of SG Snubber elimination and revised Replacement Steam Generators (RSG) weight and center of gravity (CG). This work was documented in WCAP-13206, Revision 1 [1]. The same loads and analytical methods will be used here.

Leak rate calculations were made as a function of crack length for the Alloy 182 and the Type 304N stainless steel. The normal operating loads were applied [1], in these calculations. The crack opening areas were estimated using the method of Tada, and the leak rates were calculated using a two-phase flow formulation described in [1]. The material properties of References [1], [12], and [13] were used for these calculations.

Circumferential Flaws

[

]^{a,c,e}

The fracture assessment was carried out for both the stainless steel and Alloy 182 materials. Both the Alloy 182 and the Type 304N stainless steel are known to have very high fracture toughness, and there are no known mechanisms, which could degrade the toughness during service. The calculations carried out here are intended to produce a best estimate of the critical flaw size, which will be compared to a similar best estimate of the flaw size to produce a leak rate of 10 gpm. There are conservatisms in the critical flaw size calculations, but no other overt conservatisms were applied.

Rapid, nonductile failure is possible for ferritic materials at low temperatures, but is not applicable to stainless steels. In stainless steel materials, the higher ductility leads to two possible modes of failure, plastic collapse or unstable ductile tearing. The second mechanism can occur when the applied J integral exceeds the J_{Ic} fracture toughness, and some stable tearing

occurs prior to failure. If this mode of failure is dominant, the load carrying capacity is less than that predicted by the plastic collapse mechanism.

The determination of the critical flaw length for a through-wall flaw was done using the methodology of Section XI, Appendix C [8], which is applicable for both materials. This methodology has been extended to through-wall flaws in Code Case N513 [8], which is entitled: "Evaluation Criteria for Temporary Acceptance of Flaws in Class 3 Piping." This code case has been accepted for use by the NRC in 10CFR50.55A, as issued in November of 1999. Although this code case is used for the justification for operation on moderate energy systems with through-wall flaws, it provides a useful calculational tool for through wall flaws in any piping system.

The critical flaw sizes of paragraph IWB 3640 [2] for the high toughness base materials were determined based on the knowledge that plastic collapse would be achieved and would be the dominant mode of failure.

The results of the fracture assessment are shown in Table 6-1, for both stainless steel and Alloy 182 materials. The results show very large critical flaw sizes for both materials, for both normal/upset and emergency/faulted conditions. Both materials have such high fracture toughness that failure is governed by the plastic collapse, which is governed by the material yield and ultimate tensile strength. The results are slightly better for the Alloy 182, because the tensile properties are slightly higher.

Fracture calculations have shown that a very large, through-wall flaw would be required to cause failure in the region of the cracking in hot leg A at the Virgil C. Summer Plant, Calculations were completed for both the Alloy 82/182 weld and the stainless piping, for completeness. For the Alloy 82/182 weld region, the critical length of a circumferential through wall flaw is about 44 inches long, and for an axial flaw the critical length is 35 inches. For the stainless steel, the corresponding numbers are 41 inches for a circumferential flaw, and 26 inches for an axial flaw. The results show a margin of over 6 between the size flaw to yield a leak rate of 10 gpm, and the critical length for the Alloy 182 weld metal, as well as the stainless piping, when the LBB requirement is a minimum of 2.0.

Axial Flaws

[

]^{a,c,e} This provides a margin greater than 6.0 between the flaw which would yield detectable leakage (10 gpm) and the flaw which could cause failure of the pipe. Again, the margin far exceeds the minimum requirement of 2.0.

Conclusions

The above results show that leak before break is clearly applicable for V. C. Summer. The recent leak found in loop A has demonstrated that it actually will occur in practice.

[

]^{a,c,e}

Table 6-1 Results of Fracture Assessment				
Condition	Critical Length - Stainless Steel		Critical Length – Alloy 182	
	Circumferential	Axial	Circumferential	Axial
Normal	[			
Faulted				]^{a,c,e}

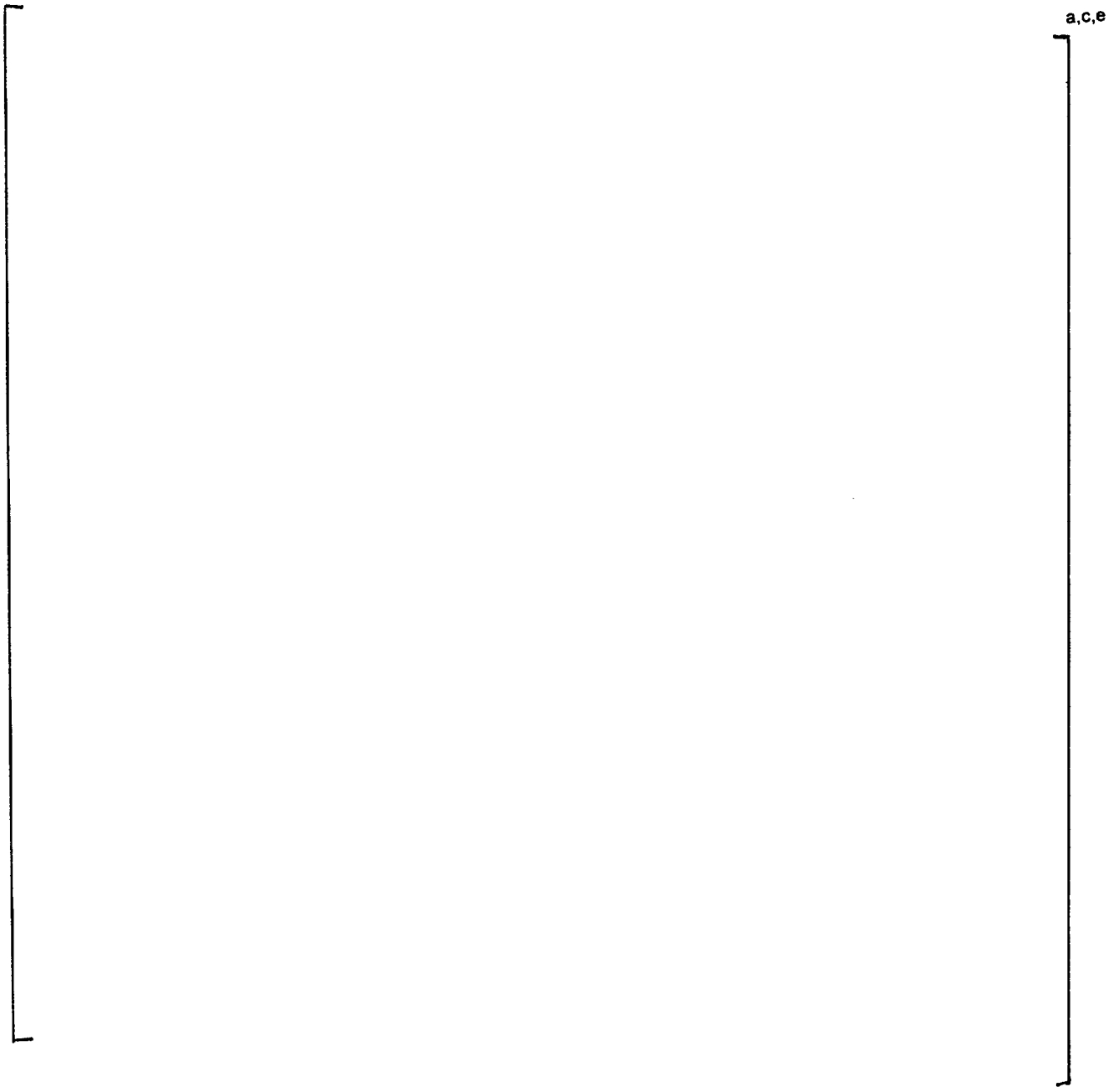

Figure 6-1 Leak Rate as a Function of Through-wall Flaw Length for V. C. Summer at 619°F

7 CONCLUSIONS

The cracked region of hot leg A has been replaced, and there are no indications in the remaining portion of loop A hot leg. An ultrasonic testing (UT) examination of the remaining nozzle to pipe welds in all the loops has found no flaws, so the plant is qualified to return to service according to the rules of Section XI.

Fracture calculations have shown that a very large, through-wall flaw would be required to cause failure in the region of the cracking in hot leg A at the Virgil C. Summer Plant, Calculations were completed for both the Alloy 182 weld and the stainless piping, for completeness. For the Alloy 182 weld region, the critical length of a circumferential through wall flaw is about 44 inches long, and for an axial flaw the critical length is 35 inches. For the stainless steel, the corresponding numbers are 41 inches for a circumferential flaw, and 26 inches for an axial flaw.

A through-wall axial flaw 2.2 inches long in the Alloy 182 weld would be expected to leak at a rate equal to the technical specification limit of 1.0 GPM, while the corresponding length for the stainless steel is 1.9 inches. This provides a very generous margin between the flaw which would yield detectable leakage and the flaw which would cause failure of the pipe.

There is concern raised as a result of a flaw discovered by eddy current testing in the loop A hot leg which had not been found by UT. Several eddy current indications were found in the other loops, and so these potential indications were addressed by a fracture analysis using the rules of ASME Section XI. The results showed that a flaw depth of 75 percent of the wall thickness would be allowable. Flaws were postulated in the unrepaired portions of the primary loops, based on the eddy current examinations of those regions, even though there were no UT indications. It has been shown that axial and circumferential flaws of the sizes measured in the hot and cold legs will be limited in size to less than the code allowable until the next inspection. Although the detection of stress corrosion racking in loop A violates one of the specified requirements for leak before break, the fact that a large LBB margin exists, and that the postulated indications will remain acceptable to Section XI, ensures that the principle of leak before break will remain valid for at least the 3.2 years of operation allowed by Section XI.

Therefore, it may be concluded that the V.C. Summer plant is in a condition that is acceptable for return to power. It is unlikely that there are indications of concern anywhere in the primary system, but if there were any, or any developed, the plant should remain in an acceptable state for at least three years.

8 REFERENCES

1. Bhowmick, D. C., "Technical Justification for Eliminating Large Primary Loop Pipe Rupture as the Structural Design Basis for the V. C. Summer Nuclear Power Plant." Westinghouse Electric Report WCAP 13206 Rev. 1, June 2000.

2. ASME Boiler and Pressure Vessel Code, Section XI, 1998 edition.

3. "Evaluation of Flaws in Austenitic Steel Piping," Trans ASME, Journal of Pressure Vessel Technology, Volume 108, August 1986, pp. 352-366.

4. "V. C. Summer Reactor Vessel Outlet Nozzle to Pipe and Inlet Nozzle to Elbow Welds: Eddy Current Examination Summary Report," Rev. 2, Westinghouse Letter Number CGE-00-109, December 7, 2000.

5. Rao, G. V., "Metallurgical Investigation and Root Cause Assessment of Cracking of Loop A Hot Leg Nozzle to Pipe Weld at V. C. Summer: Preliminary Findings Summary," Westinghouse Letter CGE-00-019, December 4, 2000.

6. Bamford, W. H. and Foster, J. P., "Crack Growth of Alloy 182 Weld Metal in PWR Environments," (PWRMRP-21), EPRI Technical Report 1000037, June 2000 (EPRI Proprietary).

7. W. H. Bamford and J. P. Foster, "Crack Growth and Microstructural Characterization of Alloy 600 PWR Vessel Head Penetrations," EPRI-TR-109136, Final Report, December 1997.

8. ASME Code Case N513, "Evaluation Criteria for Temporary Acceptance of Flaws in Class 3 Piping," approved 8/14/97.

9. WCAP-13206, "Technical Justification for Eliminating Large primary Loop Pipe rupture as the Structural Design Basis for the Virgil C. Summer Nuclear Power Plant," dated April 1992.

10. NRC Docket No. 50-395 dated January 11, 1993, "Safety Evaluation of Request to use Leak-Before-Break for Reactor Coolant System Piping – Virgil C. Summer Nuclear Station Unit No. 1 (TAC No. M83971)."

11. WCAP-13605, "Primary Loop Leak-Before-Break Reconciliation to Account for the Effects of Steam Generator Replacement/Uprating," dated March 1993.

12. ASME Code Section III, Appendices, 1989 Edition.

13. Personal Communication: David Parker of INCO Welding Products to Charles Kim, Westinghouse, October 19, 2000.

14. Barbier, C., "Yearly Review of Cycle Count from WESTEMS, Engineers Work Record CB15053," V. C. Summer Nuclear Plant, October 27, 1999.

15. James, L. A., "Fatigue Crack Propagation Behavior of Inconel 600," in Hanford Engineering Labs Report HEDL-TME-76-43, May 1976.

16. Hale, D. A. et al., "Fatigue Crack Growth in Piping and RPV Steels in Simulated BWR Water Environment," Report GEAP 24098/NUREG-CR-0390, General Electric Co., January 1978.